Electron Spin Resonance Evidence of the Generation of Superoxide Anion, Hydroxyl Radical and Singlet Oxygen during the Photohemolysis of Human Erythrocytes with Bacteriochlorin a

Maryse Hoebeke*[1], Hans J. Schuitmaker[2], Lies E. Jannink[2], Tom M. A. R. Dubbelman[3], Andreas Jakobs[1] and Albert Van de Vorst[1]

[1]Institute of Physics, University of Liège, Liège, Belgium and
[2]Department of Ophthalmology and [3]Department of Medical Biochemistry, State University of Leiden, Leiden, the Netherlands

ABSTRACT

Photodynamic therapy with bacteriochlorin a (BCA) as sensitizer induces damage to red blood cells in vivo. To assess the extent of the contributuion of reactive oxygen species (ROS) and to determine a possible reaction mechanism, competition experiments with assorted ROS quenching or/and enhancing agents were performed in human erythrocytes as model system and in phosphate buffer. In the erythrocyte experiments, a 2% suspension was incubated with BCA for 1 h, washed with phosphate-buffered saline, resuspended and subsequently illuminated with a diode laser using a fluence rate of 2.65 mW/cm^2. Potassium leakage and hemolysis were light and BCA dose dependent. Adding tryptophan (3.3 mM), azide (1 mM) or histidine (10 mM) to the erythrocyte suspension before illumination delayed the onset of K-leakage and hemolysis suggesting a type II mechanism. The D$_2$O did not affect K-leakage nor photohemolysis. Adding mannitol (13.3 mM) or glycerol (300 nM) also caused a delay in the onset of K-leakage and hemolysis, suggesting the involvement of radicals. In phosphate buffer experiments, it was shown using electron spin resonance (ESR) associated with spin-trapping techniques that BCA is able to generate $O_2^-\cdot$ and $OH\cdot$ radicals without production of aqueous electron. Visible or UV irradiation of the dye in the presence of the spin trap 5,5-dimethyl-1-pyrroline-N-oxide (DMPO) gave an ESR spectrum characteristic of the DMPO-hydroxyl radical spin adduct DMPO-OH. Addition of ethanol or sodium formate produced supplementary hyperfine splittings due to the respective $CH_3CHOH\cdot$ and $CO_2^-\cdot$ radical adducts, indicating the presence of free $OH\cdot$. Production of DMPO-OH was partly inhibited by superoxide dismutase (SOD), catalase and desferrioxamine, suggesting that the iron-catalyzed decomposition of H_2O_2 was partly involved in the formation of one part of the observed $OH\cdot$. The complementary inhibition of DMPO-OH production by azide and 9,10-anthracenedipropionic acid (ADPA) was consistent with $^1O_2$ production by BCA followed by reaction of $^1O_2$ with DMPO and decay of the intermediate complex to form DMPO-OH and free $OH\cdot$. All our results seem to indicate that BCA is a 50%/50% type 1/type 2 sensitizer in buffered aqueous solutions and confirmed that the dye-induced hemolysis of erythrocytes was well caused by a mixed type 1/type 2 mechanism.

INTRODUCTION

Photodynamic therapy (PDT)† is based on the attractive basic concept of combining two therapeutic agents, harmless by themselves, to obtain selective tumor destruction. In practice, the advance of this therapeutic modality has been hampered by unsatisfactory selectivity and serious side effects of the photosensitizer Photofrin. This prompted intense research on second-generation photosensitizers of which bacteriochlorin a (BCA) is a typical example.

Bacteriochlorin a is a relatively new photosensitizer with an absorption maximum at 760 mn and a high molar absorption coefficient of 32 000 M^{-1} cm^{-1}. At 760 nm, tissue penetration of light is optimal (1). It is an effective photosensitizer in vitro (1) and shows preferential tumor tissue retention in hamster Greene melanoma, rhabdomyosarcoma, RIF and mammatumors (2–6). The fluorescence of BCA is detectable in vivo in small solid tumors thus enabling tumor detection (4,5). In vivo, upon illumination, BCA induces tumor necrosis through vascular and direct cellular effects (2,3,5). At the dosages used to induced photodynamic effects, no adverse effects of BCA are observed in mice, rats, hamsters and rabbits (2–9). Van Iperen et al. (7) have shown

---

†Abbreviations: ADPA, anthracene dipropionic acid; BCA, bacteriochlorin a; DMPO, 5,5-dimethyl-1-pyrroline-N-oxide; DMPO-N$_3$, azide spin adduct; DMPO-OH, hydroxyl radical spin adduct; DMPO-OOH, superoxide anion spin adduct; ESR, electron spin resonance; NaN$_3$, sodium azide; $O_2^-\cdot$, superoxide anion; $^1O_2$, singlet oxygen; $OH\cdot$, hydroxyl radical; PBS, phosphate-buffered saline; PDT, photodynamic therapy; ROS, reactive oxygen species; SOD, superoxide dismutase; TLC, thin-layer chromatography.

that BCA-PDT is able to induce nonspecific systemic immune suppression.

Evidence is accumulating that the generation of reactive oxygen species (ROS) is intimately associated with the photodynamic effect of many sensitizers involved in cancer therapy. A light-activated sensitizer can transfer energy from its triplet state by two processes, directly to molecular oxygen with generation of singlet oxygen ($^1O_2$) (type 2 reaction) or by interaction with solvent or substrate by electron or proton transfer with generation of radicals (type 1 reaction). While $^1O_2$ is believed to be the major mediator of photochemical cell damage for many types of photosensitizers, oxygen species like the superoxide anion (O_2^-•) and the hydroxyl radical (OH•) can also induce deleterious effects including lipid peroxidation and membrane damage (10,11). In view of the capacity of BCA to generate $^1O_2$, already reported by Beems et al. (1), it appeared worthwhile to determine the exact nature of the oxygen species produced by the dye in order to understand its action mechanism.

In previous experiments (5) it was found that PDT with this sensitizer induced damage to erythrocytes in vivo. In the present study, this phenomenon was investigated in vitro using BCA-induced photohemolysis in human erythrocytes as a model system and assorted ROS-quenching or -enhancing agents. It was found that BCA-induced hemolysis of erythrocytes was probably caused by a mixed type 1/type 2 mechanism without a predominant role for either mechanism. To determine a contingent mechanism of ROS production, electron spin resonance (ESR) associated with spin-trapping techniques was used in phosphate buffer. The experiments indicated that BCA is a 50%/50% type 1/type 2 sensitizer. This result correlates well with the in vitro experiments indicating that both mechanisms contributed approximately equally to the BCA-PDT-inflected membrane damage.

MATERIALS AND METHODS

Chemicals. Bacteriochlorophyll *a* was purchased from Sigma or extracted from the anaerobic photosynthetic bacterium *Rhodospirillum rubbum.* Purity of the extracted bacteriochlorophyll *a* was evaluated using thin-layer chromatography (TLC). Using an eluent of 93% methanol and 7% phosphate buffer (pH 7, 10 mM), bacteriochlorophyll *a* yielded a single blue spot on Machery-Nagel Nano-Sil C_{18}-100 TLC plates (Düren, Germany). From this starting material, the photosensitizer BCA was obtained and purified as described previously (2). The BCA was stored under nitrogen in the dark at $-20°C$ until used.

Superoxide dismutase (SOD, bovine erythrocytes), catalase (bovine liver), cytochrome *c* (horse heart) and desferrioxamine were purchased from Sigma Chemical Co., sodium formate and sodium benzoate from UCB, and 5,5-dimethyl-1-pyrroline-*N*-oxide (DMPO) from Aldrich Chemical Co. The DMPO was carefully purified as described previously (12) and stored at $-20°C$ under nitrogen to avoid any oxidation of the spin trap before irradiation in the presence of the sensitizer. 9,10-Anthracenedipropionic acid (ADPA) was synthesized as described by Gandin et al. (13). All other chemicals were of analytical grade and used without purification.

Illumination of erythrocytes. The continuously stirred cell suspension was exposed to near infrared light from a custom-made laser diode (Philips, the Netherlands) with a maximun continuous wave emission of 400 mW at 757 nm. The erythrocyte suspension was irradiated at room temperature (unless otherwise stated) in open glass vessels. The light fluence rate at the surface of the cell suspension was 26.5 W m ^{2}. Light fluence was measured with a Gentec TPM-310 analog power meter (Gentec Inc., Quebec, Canada).

Photohemolysis assays. In all experiments a 2% (vol/vol) erythrocyte suspension (blood was obtained from healthy volunteers) was

incubated with BCA at room temperature for 1 h, washed twice with phosphate-buffered saline (PBS), resuspended in PBS and subsequently illuminated (continuously or for 10 min) with a fluence rate of 2.65 mW/cm². For hemoglobin and potassium determinations, samples were taken during and after illumination and spun down in an Eppendorf table centrifuge. Hemoglobin in the supernatant was determined by measuring the absorbance at 540 nm using a Beckman spectrophotometer. Potassium leakage into the supernatant was determined with a Corning (Essex, England) flame photometer. Results are expressed as percentage hemolysis or K-leakage taking 100% as the absorbance/leakage obtained from a sample lysed in distilled water. Each experiment was repeated at least three times. The standard errors recorded in triplicate measurements of the same reaction mixture were less than 5%. Variations in measurements on different days were on the order of magnitude of 20%, largely depending on the different blood donors.

Absorption spectra. The absorption spectrum of BCA in phosphate buffer (pH 7.2) was recorded on a Kontron spectrophotometer (Uvikon instruments). The variation of the optical density at the maxima with dye concentration was used to check the aggregation state of BCA. Within the range of concentrations used in our ESR experiments, BCA was present as a monomer.

Photosensitization and ESR spin trapping. The ESR measurements were performed using an aqueous flat cell at 9.56 GHz of a Bruker ESP 300E spectrometer at room temperature. Unless otherwise indicated, the spectra were recorded with nonsaturating microwave power (20 mW) and a modulation amplitude of 2 G. Samples were irradiated directly inside the microwave cavity of the spectrometer using a high pressure xenon lamp (XBO 150 W, Osram GmbH) or a high pressure mercury vapor lamp (HBO 500 W, Osram GmbH). When it was necessary, a cut-off filter (Schott OG515, Germany) was used to eliminate light under 500 nm. The spin-trapping experiments were performed in phosphate buffer with a final concentration of 100 mM DMPO. For all the spin adduct production comparison experiments, the BCA concentration was maintained at a constant value. The kinetic of spin adduct generation was studied by recording an ESR spectrum every 2 min and measuring peak heights. The results of the competition reactions were expressed in percentage of the spin adduct signal intensity in the absence of the specific inhibitors selected. The error in the rate of radical generation was estimated to be 15%.

Reduction of cytochrome c. Ferricytochrome *c* (80 μM) was added to a phosphate buffer (pH 7.2) solution of BCA ($3.5 \times 10^{-5} M$) that had been previously irradiated during 30 min in a quartz spectrophotometer cell (10 mm optical path, 3 mL total volume). The reduction of ferricytochrome *c* to ferrocytochrome *c* was monitored continuously at 418 nm during 2 h and the kinetic study was started in less than 30 s from the moment of ferricytochrome *c* addition. The molar exctinction coefficient for ferricytochrome *c* at this wavelength was $0.89 \times 10^4 M^{-1} cm^{-1}$ and for ferrocytochrome *c* $2.99 \times 10^4 M^{-1} cm^{-1}$ (14).

Laser flash photolysis. Nanosecond transient absorption spectroscopy was performed using a Q-switched Nd/YAG laser (Quantel YG 441, Orsay, France). The excitation wavelength ($\lambda = 354.7$ nm, 2 ns pulse at half-maximum) was generated by frequency conversion using two nonlinear crystals (KDP). Cylindrical lenses were used to obtain a laser beam of 1 cm width and 0.4 cm height at the entrance of a 1 cm $\times$ 1 cm silica cuvette with polished windows containing the sample. A frosted silica plate in front of the entrance window was used to obtain uniform excitation of the sample. Variations in light transmission through the sample were measured using a flash lamp–monochromator–photomultiplier set-up with 2 ns time resolution and 1 nm spectral resolution. The photomultiplier signal was measured as a function of time using a digitized oscilloscopoe (Tektronic 2440) that was connected to a PC microcomputer. Transmission variations across the cuvette were measured perpendicularly to the laser beam in a volume closely adjacent to the laser entrance window. Dissolved oxygen was removed by bubbling argon for at least 30 min. Fluences were varied using Scott neutral density filters.

RESULTS

Photohemolysis

The BCA-induced photohemolysis of the 2% erythrocyte suspension is shown in Fig. 1. The K-leakage and hemolysis
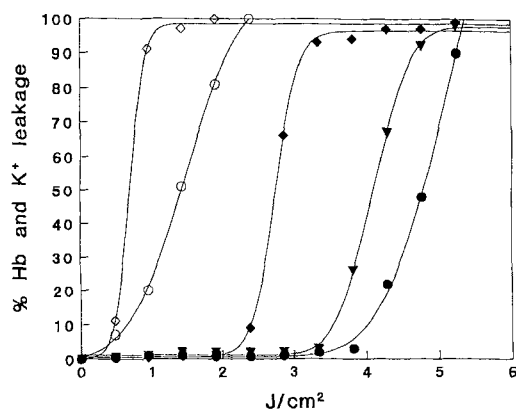
Figure 1. Concentration dependency of BCA-PDT-induced K-leakage and hemolysis expressed as % from control (erythrocytes lysed in distilled water). Photohemolysis was always preceded by K-leakage indicating the colloid-osmotic nature of the process. Open symbols: K-leakage, closed symbols: hemolysis. ●, 6 μg/mL; ▼, 9 μg/mL; ♦, 12 μg/mL; ○, 6 μg/mL; ◇, 12 μg/mL.

curves are sigmoidal which is indicative for this colloid osmotic process (15). Figure 1 also shows that the shape of the sigmoidal hemolysis curve is shifted to lower rate values when increasing the BCA concentration and does not change form. It is important to note that BCA alone, or light alone at the highest fluence rate used, did not induce photohemolysis. In addition, it should be stressed that the observed hemolysis is due to BCA on, or inside the erythrocyte as the dye was not present in the solution during or after illumination (see Materials and Methods).

To determine the extent of the involved ROS in the observed hemolysis, various quenching and enhancing agents were used. The results of these experiments are presented in Table 1. This table shows the influence of the assorted compounds on the relative rate of hemolysis. In this table, the energy (Joule) or time necessary to induce 50% hemolysis upon illumination after incubation of the 2% erythrocyte suspension with BCA was taken as 1. All type 1 and type 2 quenchers delayed the onset of hemolysis; the largest delay was obtained with tryptophan, a mixed type 1–type 2 quencher (16). BHT, a strong suppressor of lipid peroxidation (17) and SOD had no, or only a minor protective effect, making the involvement of lipid peroxidation or the $O_2^{-\cdot}$ unlikely. Also by measuring thiobarbituric acid-reactive substances we could not detect lipid peroxides after light exposure (results not shown).

Spin trapping with DMPO

In phosphate buffer (pH 7), irradiation of BCA (4 $\times$ 10^{-5} *M*) with visible light ($\lambda >$ 500 nm) or with UV light in the presence of DMPO (10^{-1} *M*) produced a four-lines ESR spectrum with hyperfine splittings (a^N = a^H = 14.9 G) characteristic of the DMPO-OH spin adduct (18,19) (Figs. 2 and 3). The signal intensity increased linearly with BCA concentration (data not shown). No signal was observed in the dark or under N$_2$ while bubbling with O$_2$ increased DMPO-OH generation. No DMPO-OOH adduct, resulting from direct $O_2^{-\cdot}$ trapping by DMPO, was observed.

The detection of an hydroxynitroxide such as DMPO-OH does not necessarily mean that OH$^\bullet$ was trapped. To check

Table 1. Effect of the addition of type 1 (mannitol, glycerol, SOD, BHT) and type 2 (azide, histidine and D$_2$O) quenchers on the *in vitro* photohemolysis of human erythrocytes*

Compound	Relative rate of photohemolysis	
	A	B
BCA only	1	1
+ Azide (1 m*M*)	1.33	1.39
+ Histidine (10 m*M*)	1.22	—
+ D$_2$O	1.02	1
+ Tryptophan (3.3 m*M*)	1.56	1.53
+ Mannitol (13.3 m*M*)	1.38	1.81
+ Glycerol (300 m*M*)	1.25	1.43
+ SOD (500 U/mL)	1.09	—
+ BHT (20 m*M*)	1.10	1.19
+ Plasma (5%)	∞	∞

*To calculate the relative rate of hemolysis, the energy (J) or time to induce 50% hemolysis after incubation with 6 μg/mL BCA was taken as 1. A = continuous illumination; B = 10 min illumination.

if freely diffusing OH$^\bullet$ was produced in the system, complementary experiments were undertaken. The inhibitors selected to compete with DMPO for OH$^\bullet$ were ethanol, sodium formate and sodium benzoate. The addition of sodium benzoate resulted in diminished production of DMPO-OH adduct, an 85% maximum inhibition being observed when sodium benzoate concentration reached 0.1 *M* (Table 2). In the presence of ethanol (2%) and sodium formate (1 *M*), the DMPO-OH spin adduct signal intensity was reduced and a new six-lines ESR spectrum corresponding respectively to the CH$_3$CHOH$^\bullet$ (a^N = 15.8 G, a^H = 22.8 G) and the CO$_2^{-\cdot}$ (a^N = 15.6 G, a^H = 18.7 G) radical trapping appeared (Fig. 2) (20). These competitive scavenging results clearly indicated the formation and the trapping of freely diffusing OH$^\bullet$ during the irradiation of BCA in the presence of DMPO. The mechanism of radical production remains to be clarified, the origin of the DMPO-OH not resulting from OH$^\bullet$ trapping must be examined together with the role of DMPO itself in spin adduct production. The lack of DMPO-OOH spin adduct signal observation did not exclude the production of $O_2^{-\cdot}$ at one step of the mechanism. Indeed, the ESR detection of DMPO-OOH is not without difficulties because of the short lifetime of the adduct and its possible decay to form DMPO-OH (21,22). To assess the possible generation of $O_2^{-\cdot}$ during the photosensitization process, the effect of SOD was investigated on DMPO-OH formation. The addition of this enzyme (100 U mL^{-1}) prior to illumination decreased the amount of DMPO-OH signal intensity to 50% of its value without SOD (Table 2), whereas thermally denatured SOD had no effect on the ESR spectrum. Increasing the SOD concentration above 100 U mL^{-1} did not change the percentage of observed DMPO-OH reduction. Although the spin trapping was the most currently used method to detect the involvement of $O_2^{-\cdot}$ in a photosensitizing process, this radical species could also be characterized by its reaction with ferricytochrome *c* leading to ferrocytochrome *c* (23). The irradiation of a phosphate buffer (pH 7.2) solution of BCA led to the spectrophotometric reduction of ferricytochrome *c* (80 μ*M*), the increase of absorbance at 550 nm being characteristic of the formation of ferrocytochrome *c*.
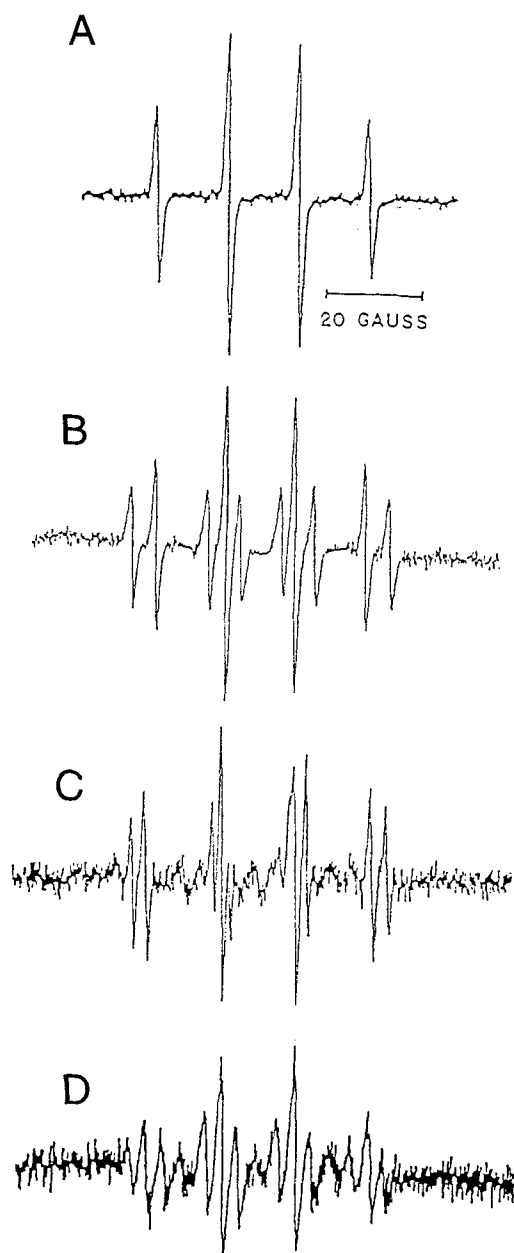
A

20 GAUSS

B

C

D

Figure 2. The ESR spectra of spin-trapped radicals obtained by irradiation of BCA (4 × 10^{-5} M) plus DMPO (10^{-1} M) (a) under air, (b) in the presence of HCOONa (1 M), (c) in the presence of 2% ethanol and (d) in the presence of NaN$_3$ (5 × 10^{-2} M).

Control experiments indicated that BCA, oxygen and light were essential for the reduction of ferricytochrome c. Thus, this method gave results consistent with the ESR experiments demonstrating the formation of O_2^- $^\bullet$ by BCA.

In order to check the eventual role of a photoejection mechanism in the pathway to produce O_2^- $^\bullet$, the sample containing DMPO and BCA was irradiated under N$_2$O. When O$_2$ was replaced by this gas that converts hydrated electrons to OH$^\bullet$ radicals (18), no DMPO-OH spin adduct was detected. The absence of photoejected electron was confirmed by a laser flash photolysis experiment. The absorbance variations following the laser excitation of an argon-saturated 5
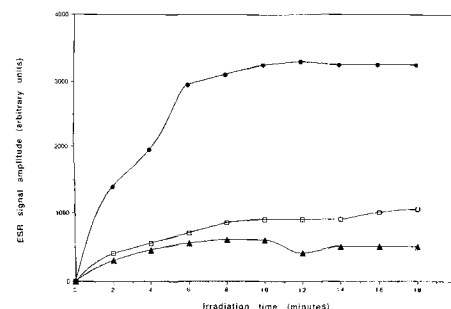

Figure 3. The DMPO-OH adduct apparition as a function of irradiation time at different BCA concentrations (-●-, 3.6 × 10^{-5} M; -□-, 1.5 × 10^{-5} M; --▲-, 0.7 × 10^{-5} M).

× 10^{-5} M aqueous solution of BCA were monitored at 715 nm. Whatever the laser fluences selected between 10 and 100 μJ, no absorbance change was observed at the absorption maximum of the hydrated electron.

Knowing that O_2^- $^\bullet$ was involved in the OH$^\bullet$ generation, its participation to a Haber–Weiss type reaction has to be investigated. A maximum 50% DMPO-OH reduction similar to that obtained with SOD was observed when catalase (500 μg/mL) or desferrioxamine (500 μM) was added to the BCA solution (Table 2). Heat-inactivated catalase was without effect. The partial inhibitory activity of catalase that removes hydrogen peroxide and desferrioxamine, which is reported as being a highly Fe^{3+} chelator, suggested that the iron-catalyzed decomposition of H$_2$O$_2$ was involved in the formation of one part of the observed OH$^\bullet$.

An explanation remained to be found for the plateau reached by SOD, catalase and desferrioxamine inhibition arising at 50% of the decrease. The DMPO, which is widely used to provide evidence for the involvement of free radicals in many biological and chemical reactions, is also able to interact with ^{1}O$_2$ to give at last an ESR spectrum corresponding to the OH$^\bullet$ adduct (24,25). This actually well-known property of the nitrone spin trap DMPO led us to suspect a ^{1}O$_2$ intermediary in the formation of DMPO-OH. To check this hypothesis, sodium azide (NaN$_3$) and anthracene dipropionic acid (ADPA) were used as ^{1}O$_2$ quenchers in competition experiments. In the presence of NaN$_3$, the ESR spectrum showed a simultaneous reduction of the DMPO-OH adduct (Fig. 2) and the formation of the DMPO-N$_3$ adduct consisting of a quartet of triplets (a^H = 14.9 G, a^{N1} = 14.9 G, a^{N2} = 3 G) (26). When the NaN$_3$ concentration in the

Table 2. Relative intensity of the DMPO-OH signal intensity during BCA irradiation in the presence of inhibitors

	Concentration	DMPO-OH reduction (%)
Sodium benzoate	0.1 M	85
SOD	100 U/mL	47
Heat-inactivated SOD	100 U/mL	0
Catalase	500 μg/mL	50
Heat-inactivated catalase	500 μg/mL	0
Desferrioxamine	500 μM	50
Sodium azide	10^{-2} M	85
ADPA	75 μM	50

solution was increased to 10^{-2} M, an 85% DMPO-OH reduction was observed (Table 2). In the presence of ADPA (75 μM), the visible irradiation of the BCA solution led to a maximum 50% reduction of the DMPO-OH spin adduct obtained in the absence of ADPA and at the same excitation conditions (Table 1). All these results confirmed the capacity of BCA to generate $^1O_2$ as already reported by Beems *et al.* (1).

DISCUSSION

In all experiments, BCA-induced photohemolysis was preceded by K-leakage from the erythrocytes, indicating the colloid osmotic nature of this process (16). Azide and histidine both delayed the onset of K-leakage and hemolysis, suggesting a type 2 mechanism and thus the involvement of $^1O_2$. In D_2O, the excited singlet lifetime of oxygen is increased approximately 10 times (15). If BCA-mediated photohemolysis is induced *via* a type 2 mechanism, an increased induction of K-leakage and hemolysis can be expected in D_2O solutions. In our experiments, D_2O did not enhance the onset of photohemolysis, arguing against the involvement of $^1O_2$. However, the possibility should be considered that $^1O_2$ is generated on/in a location where D_2O cannot exert any effects, *e.g.* inside the erythrocyte membrane. Bacteriochlorin *a* is a hydrophobic sensitizer, and one may assume that it localizes in a hydrophobic region that is not accessible to water. On the other hand, one should also consider the possibility that the increased lifetime of $^1O_2$ due to D_2O does not result in more damage to the membrane of the erythrocyte because $^1O_2$ leaves the membrane to react with hemoglobin. In this respect it must be emphasized that BCA was not present in the erythrocyte suspension during and after illumination. As hemolysis always occurred, one may conclude that exogenous BCA is not required for hemolysis and that BCA bound to or inside the erythrocyte is responsable for the observed effects.

Mannitol and glycerol, known scavengers of hydroxyl radicals (16), both delayed the onset of BCA-induced photohemolysis, suggesting the involvement of radicals. The largest delay in the onset of hemolysis was obtained with tryptophan. Tryptophan rapidly reacts with $^1O_2$ and OH•.

Summarizing, the results of the erythrocyte experiments suggest that BCA-induced photohemolysis is a colloid osmotic process and that the inflicted membrane damage is probably the result of a mixed type 1/type 2 mechanism. From the results obtained, a predominant role for either mechanism cannot be ascertained, therefore additional ESR experiments were performed.

The ESR spin-trapping experiments showed that BCA could generate a DMPO-OH spin adduct upon visible or UV irradiation. There are a number of potential sources for this signal other than freely diffusing OH• trapping by DMPO such as (24): (1) a direct interaction between light-actived BCA and the spin trap, (2) the production of O_2^-• followed by trapping of O_2^-• by DMPO and decay of DMPO-OOH signal to DMPO-OH, (3) production of O_2^-• in a Haber–Weiss reaction leading to OH• formation and (4) formation of a complex between DMPO and $^1O_2$ and its subsequent decay to DMPO-OH and free OH•.

The absence of a DMPO-OH signal under N_2 and its enhancement under O_2 showed firstly the importance of molecular oxygen in the mechanism and secondly made impossible a direct interaction between BCA and DMPO to be the source of DMPO-OH.

The best way to prove the existence of freely diffusing OH• in a system was to perform competition experiments with OH• scavengers. Using a kinetic approach (27) the relative efficiency of radical scavengers such as sodium benzoate (0.1 M) and DMPO (10^{-1} M) was quantitatively predictable from the known rate constants for reactions of the OH• radical with the compound, respectively k_1 (6 × 10^9 dm^3 mol^{-1} s^{-1}) and k_2 (4.3 × 10^9 dm^3 mol^{-1} s^{-1}) (27,28). The 88% maximum inhibition observed in our experiment when sodium benzoate reached 0.1 M was consistent with the predicted calculated value (85%). Moreover, further evidence on free OH• production in the system was obtained by carrying out the BCA irradiation in the presence of ethanol and sodium formate. A new signal corresponding to the hydroxyethyl adduct or the CO_2^-• adduct was observed in concordance with the DMPO-OH decrease. All these results clearly indicated that freely diffusing OH•, able to react with these well-known OH• scavengers, were generated in the system. But, at this stage of our study, the investigation of the OH• mechanism generation was to be continued.

The formation of the DMPO-OH spin adduct inhibited by SOD (Table 2), a specific O_2^-• catalytic substrate, implied that OH• radical formation was dependent on O_2^-• in a Fenton reaction, for example, or that O_2^-• was trapped first and the resulting O_2^-• adduct was reduced to form OH• adduct. The DMPO-OOH adduct could also decompose slowly to release OH•. The absence of a visualized DMPO-OOH spin adduct could be the result of a too low O_2^-• steady-state concentration resulting in the implication of this radical species in the Fenton chemistry or in the short lifetime of this very unstable spin adduct in water, especially in the presence of transition metals (20–22). Because a Fenton reaction required H_2O_2, catalase was introduced in the system before irradiation. Its ability to decrease the intensity of the ESR signal in a way similar to SOD (Table 2) demonstrated that H_2O_2 was involved in the mechanism of OH• production. Desferrioxamine was then included to chelate any residual Fe^{3+}, and its addition led also to a DMPO-OH reduction (Table 1). The parallel observed effect of SOD, catalase and desferrioxamine suggested that O_2^-• can react with H_2O_2 to generate OH• *via* the Haber–Weiss reaction catalyzed by iron:

$$Fe^{3+} + O_2^- \text{•} \rightarrow Fe^{2+} + O_2$$
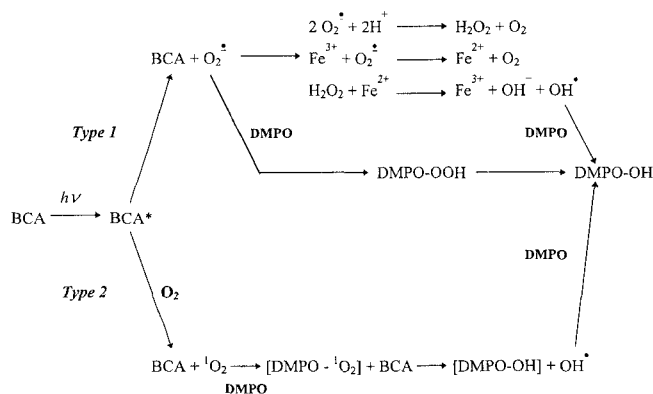
$$Fe^{2+} + H_2O_2 \rightarrow Fe^{3+} + OH^- + OH\text{•}$$
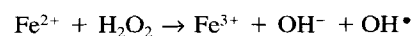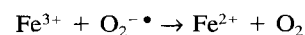
Moreover, the production of O_2^-• by photoexcited BCA was also characterized and then confirmed by its reaction with ferricytochrome *c* leading to the single known product ferrocytochrome *c* for which the formation kinetics can be spectrophotometrically followed. Thus all the experimental results are consistent with the existence of O_2^-• as an intermediate species able to produce free OH•.

In an attempt to identify the pathway of O_2^-• formation, the eventual ejection of electrons, able to become hydrated electrons (e_{aq}) before reacting with molecular oxygen, was tested. When air was replaced by N_2O, which converts e_{aq}

to OH$^\bullet$ with a constant rate of 9×10^9 M^{-1} S^{-1} (18), no DMPO-OH signal was observed. This result combined with the absence of DMPO-H adduct led us to rule out the participation of e_{aq} to $O_2^{-\bullet}$ formation. The lack of e_{aq} production during BCA excitation was also verified by laser flash photolysis experiments.

At this step of the study, the inability of SOD, catalase and desferrioxamine to inhibit more than 50% of the hydroxyl radical adduct formation had to be elucidated. Indeed, if $O_2^{-\bullet}$ was trapped, then the formation of the DMPO-OH radical adduct might be inhibited by SOD. The plateau reached at about 50% of the decrease was a good indication that another mechanism was occurring. Singlet oxygen-mediated oxidation of DMPO to radical species is actually well documented (20–22,24,25). Reaction of $^1O_2$ with DMPO was reported to give a complex followed by decay to DMPO-OH and free OH$^\bullet$, which might be then trapped by DMPO or scavenged by ethanol, sodium formate or sodium benzoate. Thus, the observation of OH$^\bullet$ radical adduct might indicate $^1O_2$ generation by BCA rather than OH$^\bullet$ production. The best way to prove the existence of $^1O_2$ in a system was to perform a competition experiment with a $^1O_2$ scavenger. Sodium azide is one of the most currently used quenchers to test for $^1O_2$ involvement (13,20). However, it is well known that azide anions can also react with OH$^\bullet$ radicals to generate $N_3^\bullet$ ($k_{NaN3+OH\bullet} = 10^{10}$ M^{-1} S^{-1}) that may then be trapped by DMPO (22,26). When the NaN_3 concentration in the reaction mixture was increased to 5×10^{-2} M, the ESR spectrum of the DMPO-N_3 spin adduct gradually appeared (Fig. 1) at the same time that the DMPO-OH signal decreased. Nevertheless, the final inhibition of DMPO-OH could not be attributed only to the free OH$^\bullet$ trapping by NaN_3. Indeed, using literature rate constants for the competition between DMPO (1 M) and NaN_3 (5×10^{-2} M), a 23% inhibition was calculated instead of the 80% observed experimentally. The reaction of NaN_3 with $^1O_2$ leading to nonparamagnetic species could explain this difference (25). The reduction of the DMPO-OH signal in the presence of ADPA (Table 2), a more specific $^1O_2$ quencher, confirmed the hypothesis that $^1O_2$ reacts with DMPO giving rise to an intermediate that decays to form DMPO-OH and free OH$^\bullet$ able to react with any scavenger. The final mechanism proposed for the BCA production of excited oxygen forms could be the following:

$$2\,O_2^{-\bullet} + 2H^+ \longrightarrow H_2O_2 + O_2$$
$$BCA + O_2^{-\bullet} \longrightarrow Fe^{3+} + O_2^{-\bullet} \longrightarrow Fe^{2+} + O_2$$
$$H_2O_2 + Fe^{2+} \longrightarrow Fe^{3+} + OH^- + OH^\bullet$$

$$BCA + {}^1O_2 \xrightarrow{\ DMPO\ } [DMPO - {}^1O_2] + BCA \longrightarrow [DMPO\text{-}OH] + OH^\bullet$$

The 50% maximum inhibition of DMPO-OH signal observed respectively with ADPA and SOD suggests that BCA is a 50%/50% type 1/type 2 sensitizer.

REFERENCES

1. Beems, E., T. Dubbelman, J. Lugtenburg, J. Van Best, M. Smeets and J. Boegheim (1987) Photosensitizing properties of bacteriochlorophyllin *a* and bacteriochlorin *a*, two derivatives of bacteriochlorophyll *a*. *Photochem. Photobiol.* **46**, 639–643.
2. Schuitmaker, J. J., J. A. van Best, J. L. van Delft, T. M. A. R. Dubbelman, J. A. Oosterhuis and D. de Wolff-Rouendaal (1990) Bacteriochlorin a, a new photosensitizer in photodynamic therapy: *in vivo* results. *Invest. Ophthalmology Visual Sci.* **31**, 1444–1450.
3. Schuitmaker, J. J., G. F. J. M. Vrensen, J. L. van Delft, D. de Wolff-Rouendaal, T. M. A. R. Dubbelman and A. de Wolf (1991) Morphologic effects of bacteriochlorin *a* and light *in vivo* on intraocular melanoma. *Invest. Ophthalomology Visual Sci.* **32**, 2683–2688.
4. Schuitmaker, J. J., H. L. L. M. van Leengoed, N. van der Veen, T. M. A. R. Dubbelman, W. M. Star (1993) Laser-induced *in-vivo* fluorescence of bacteriochlorin a; preliminary results. *Laser Med. Sci.* **8**, 39–42.
5. van Leengoed, H. L. L. M., J. J. Schuitmaker, N. van der Veen, T. M. A. R. Dubbelman, W. M. Star (1993) Fluorescence and photodynamic effects of bacteriochlorin a observed *in vivo* in "sandwich observation" chambers. *Br. J. Cancer* **67**, 898–903.
6. van Geel, I. P. J., H. Oppelaar, Y. G. Oussoren, J. J. Schuimaker and F. A. Stewart (1995) Mechanisms for optimizing PDT: second generation photosensitizers in combination with mitomycin C. *Br J. Cancer* **72**, 344–350.
7. van Iperen, H. P., H. J. Sctuitmaker and G. M. J. Beijersbergen van Henegouwen (1995) Non-specific systemic immune suppression induced by photodynamic treatment of lymph node cells with bacteriochlorin a. *J. Photochem. Photobiol. B Biol.* **28**, 197–202.
8. Schuitmaker, J. J., R. I. J. Feitsma, J. G. Joumee-de Korver, T. M. A. R. Dubbelman and E. K. J. Pauwels (1993) Tissue distribution of bacteriochlorin a labelled with ^{99m}Tc-pertechnetate in hamster Greene melanoma. *Int. J. Radiat. Biol.* **64**, 451–458.
9. van Best Jaap, A., H. J. Schuitmaker, T. M. A. R. Dubbelman, C. J. van der Poel, J. Fakkel (1993) Near infra-red diode laser for photodynamic therapy using bacteriochlorin a. *Laser Med. Sci.* **8**, 157–162.
10. Dolphin, D. (1994) Photomedecine and photodynamic therapy. *Can. J. Chem.* **72**, 1005–1013.
11. Kriska, T., L. Korecz, I. Nemes and D. Gal (1995) Physicochemical modeling of the role of free radicals in photodynamic therapy. III. Interactions of stable free radicals with excited photosensitizers studied by kinetic ESR spectroscopy. *Biochem. Biophys. Res. Commun.* **215**, 192–198.
12. Hoebeke, M., E. Gandin and Y. Lion (1986) Photoionisation of tryptophan: an electron spin resonance investigation. *Photochem. Photobiol.* **44**, 543–546.
13. Gandin, E., Y. Lion and A. Van de Vorst (1983) Quantum yield of singlet oxygen production by xanthene derivatives. *Photochem. Photobiol.* **37**, 271–278.
14. Sanders, S. P., S. J. Harrison, P. Kuppusamy, J. T. Sylvester and J. L. Zweier (1994) A comparative study of EPR spin trapping and cytochrome c reduction techniques for the measurement of superoxide anions. *Free Radical Biol. Med.* **16**, 753–761.
15. Rosenthal, I. and E. Ben-Hur (1995) Role of oxygen in the phototoxicity of phthalocyanines. *Int. J. Radiat. Biol.* **67**, 85–91.
16. Sonoda, M., C. M. Krishna and P. Riesz (1987) The role of singlet oxygen in the photohemolysis of red blood cells by phthalocyanine sulfonates. *Photochem. Photobiol.* **46**, 625–631.
17. van der Zee, J., T. M. A. R. Dubbelman and J. van Steveninck

(1985) Peroxide-induced membrane damage in human erythrocytes. *Biochim. Biophys. Acta* **818**, 38–44.

18. Faraggi, M., A. Carmichael and P. Riez (1984) OH radical formation by photolysis of aqueous porphyrin solutions. A spin trapping and E.S.R. study. *Int. J. Radiat. Biol.* **46**, 703–713.

19. Finkelstein, E., G. Rosen and E. Rauckman (1980) Spin trapping of superoxide and hydroxyl radical: practical aspects. *Arch. Biochem. Biophys.* **200**, 1–16.

20. Collet, M., M. Hoebeke, J. Piette, A. Van de Vorst, A. Jakobs and L. Lindqvist (1996) Photosensitized generation of hydroxyl radical by eight new sulfur and selenium analogs of psoralen. *J. Photochem. Photobiol. B Biol.* **99**, 1–999.

21. Buettner, G. (1993) The spin trapping of superoxide and hydroxyl free radicals with DMPO (5,5-dimethylpyrroline-*N*-oxide): more about iron. *Free Radical Res. Commun.* **19**, 79–87.

22. Buettner, G. and L. Oberley (1978) Considerations in the spin trapping of superoxide and hydroxyl radical in aqueous systems using 5,5-dimethylpyrroline-*N*-oxide. *Biochem. Biophys. Res. Commun.* **83**, 69–74.

23. McCord, J. and I. Fridovich (1969) An enzymic function for erythrocuprein (hemocuprein). *J. Biol. Chem.* **25**, 6049–6055.

24. Feix, J. and B. Kalyanaraman (1991) Production of singlet oxygen-derived hydroxyl radical adducts during merocyanine-540-mediated photosensitization: analysis by ESR-spin trapping and HPLC with electrochemical detection. *Arch. Biochem. Biophys.* **15**, 43–51.

25. Bilsky, P., K. Reszka, M. Bilska and C. Chignell (1996) Oxidation of the spin trap 5,5-dimethyl-1-pyrroline *N*-oxide by singlet oxygen in aqueous solution. *J. Am. Chem. Soc.* **118**, 1330–1338.

26. Kremers, W. and A. Singh (1980) Electron spin resonance study of spin-trapped azide radicals in aqueous solutions. *Can. J. Chem.* **58**, 1592–1595.

27. Mason, R., P. Hanna, M. Burkitt and M. Kadiiska (1994) Detection of oxygen-derivated radicals in biological systems using electron spin resonance. *Environ. Health Perspect.* **102**, 33–36.

28. Castelhano, A., M. Perkins and D. Griller (1982) Spin trapping of hydroxyl in water: decay kinetics for the OH and CO_2 adducts to 5,5-dimethyl-1-pyrroline-*N*-oxide. *Can. J. Chem.* **61**, 298–299.